

## Supporting Information

### **Asymmetric Side-Chain Engineering of Conjugated Polymers with Improved Performance and Stability in Organic Electrochemical Transistors**

Guo-Hao Jiang,<sup>a</sup> Chia-Ying Li,<sup>a</sup> Shang-Wen Su,<sup>a</sup> Yan-Cheng Lin,<sup>a,b,\*</sup>

<sup>a</sup>Department of Chemical Engineering, National Cheng Kung University, Tainan City  
70101, Taiwan.

<sup>b</sup>Advanced Research Center for Green Materials Science and Technology, National  
Taiwan University, Taipei 10617, Taiwan.

\*Corresponding authors. E-mail: ycl@gs.ncku.edu.tw (Y.-C. L.)

**Table S1.** Optical and electrochemical parameters of the polymer films.

Polymer	P(C,C)	P(C,O)	P(O,O)
$\lambda_{\max}$ (nm)	703	710	718
(0-0 / 0-1)	0.767	0.806	0.847
E <sub>g</sub> (eV)	1.64	1.61	1.58
HOMO (eV)	-5.52	-5.31	-5.08
LUMO (eV)	-3.88	-3.70	-3.50
$\Delta E_{\text{onset}}$ (eV)	0.202	0.606	0.695

**Table S2.** GIXD crystallographic parameters of the as-cast and electrolyte-swelled polymer films derived from the OOP line-cutting profiles.

OOP	As-cast			Swelled		
	P(C,C)	P(C,O)	P(O,O)	P(C,C)	P(C,O)	P(O,O)
$d_{200}$ (Å)	12.04	12.91	11.61	12.09	12.91	12.09
FWHM (Å)	0.089	0.063	0.054	0.092	0.067	0.040
$L_{c,200}$ (Å)	63.25	90.05	104.53	61.80	83.89	139.97
$g_{200}$	0.183	0.159	0.140	0.186	0.165	0.123

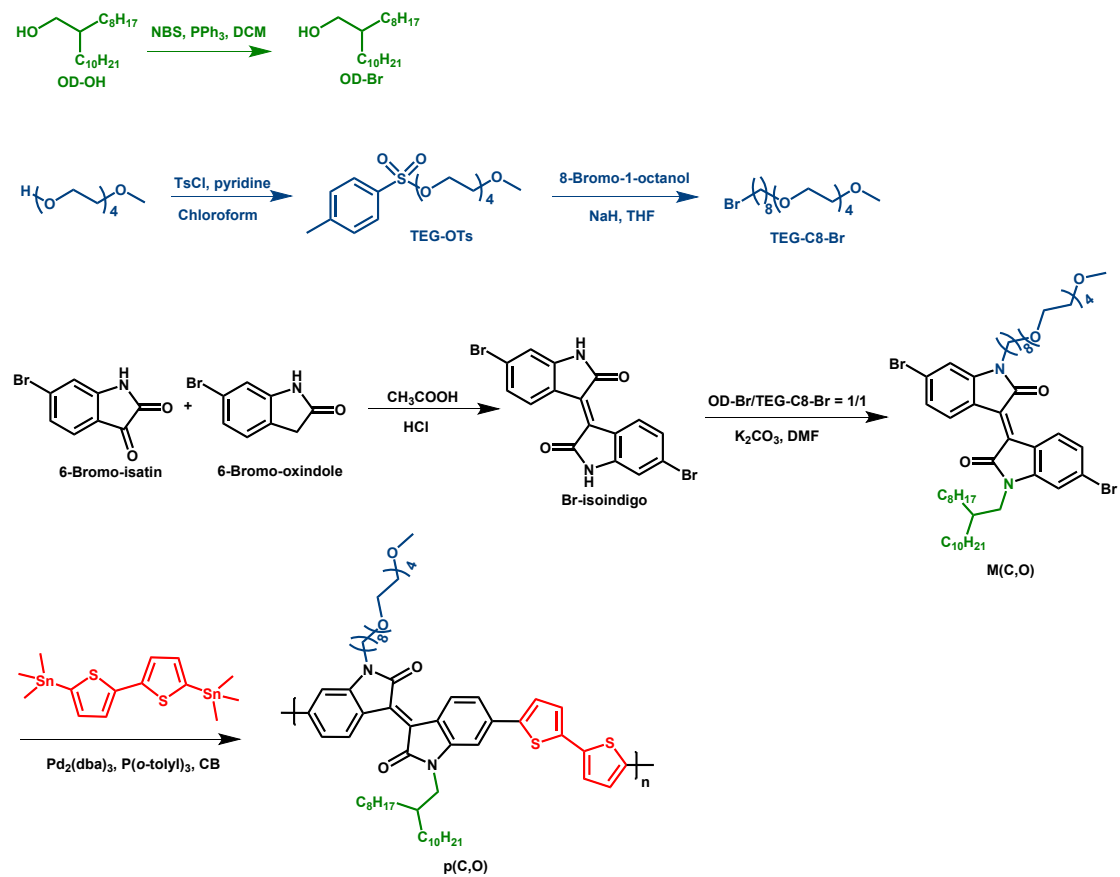
**Table S3.** GIXD crystallographic parameters of the as-cast and electrolyte-swelled polymer films derived from the IP line-cutting profiles.

IP	As-cast			Swelled		
	P(C,C)	P(C,O)	P(O,O)	P(C,C)	P(C,O)	P(O,O)
$d_{010}$ (Å)	-	3.55	3.65	-	3.55	3.67
FWHM (Å)	-	0.089	0.104	-	0.091	0.098
$L_{c,010}$ (Å)	-	63.54	54.37	-	62.14	57.70
$g_{010}$	-	0.099	0.109	-	0.100	0.106

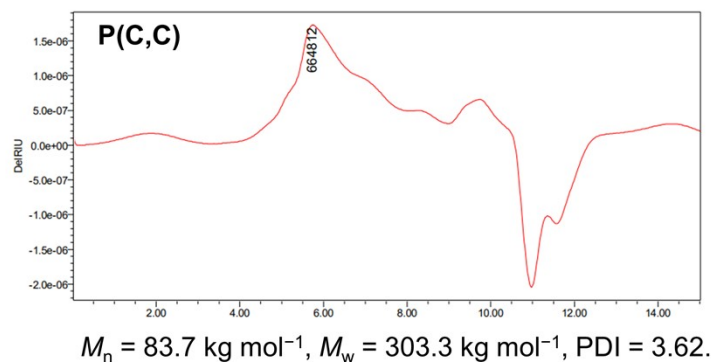
**Table S4.** GIXD crystallographic parameters of the as-cast and electrolyte-swelled polymer films derived from the geometrically corrected azimuthal integral profiles.

	As-cast			Swelled		
	P(C,C)	P(C,O)	P(O,O)	P(C,C)	P(C,O)	P(O,O)
<b>OOP area</b>	2.292	4.012	12.837	4.999	6.858	15.2
<b>IP area</b>	0.322	0.378	0.256	0.803	0.152	0.178
<b>OOP / (IP+OOP)</b>	0.877	0.914	0.980	0.862	0.978	0.988
<b>rDOC (%)</b>	15.1	26.4	84.5	32.9	45.1	100.0

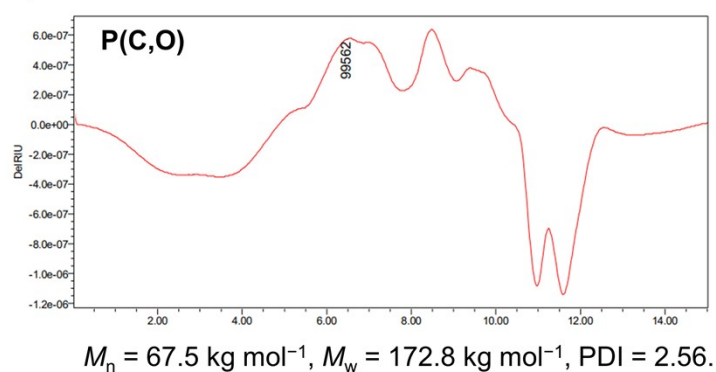
**Scheme S1.** Synthetic routes of the side chains, isoindigo monomers, and P(C,O) with asymmetric side chains.



a)



b)



c)

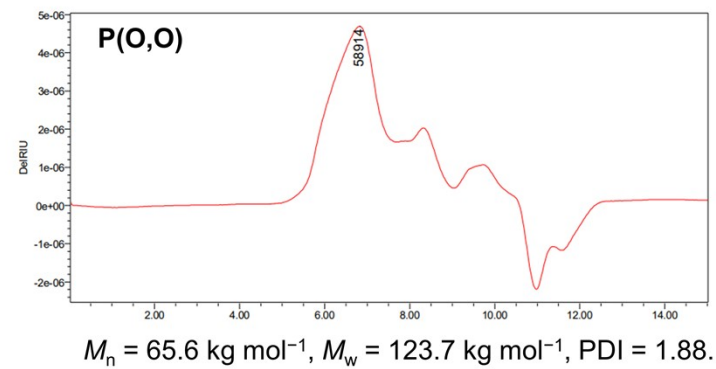


**Fig. S1.** GPC curves of (a) P(C,C), (b) P(C,O), and (c) P(O,O).

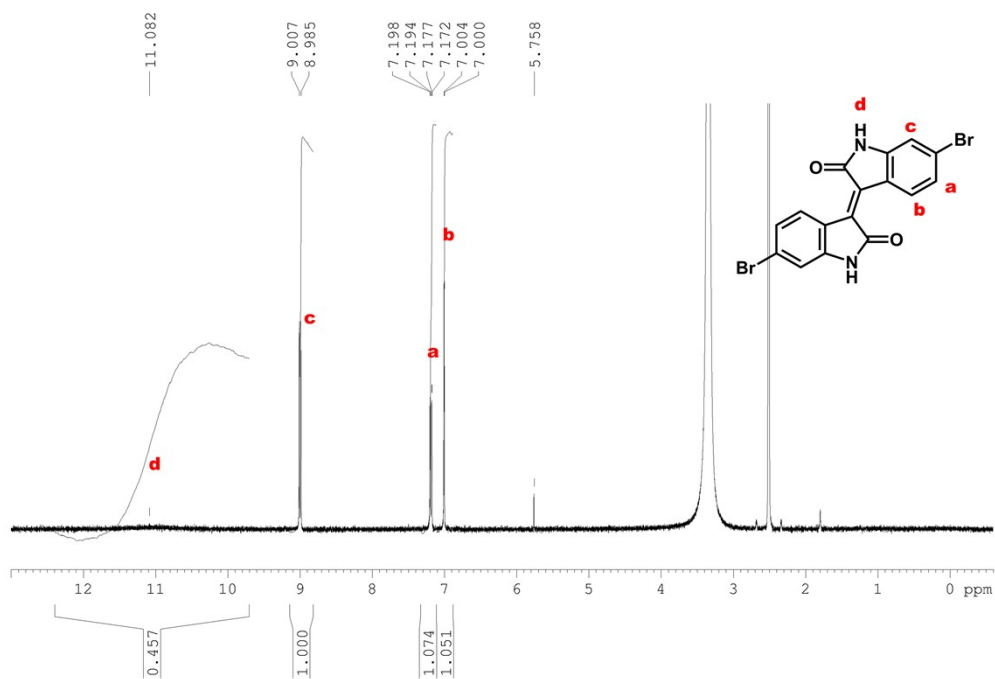


**Fig. S2.**  $^1\text{H}$  NMR spectrum of **Br-isoindigo** in  $d_6$ -DMSO.

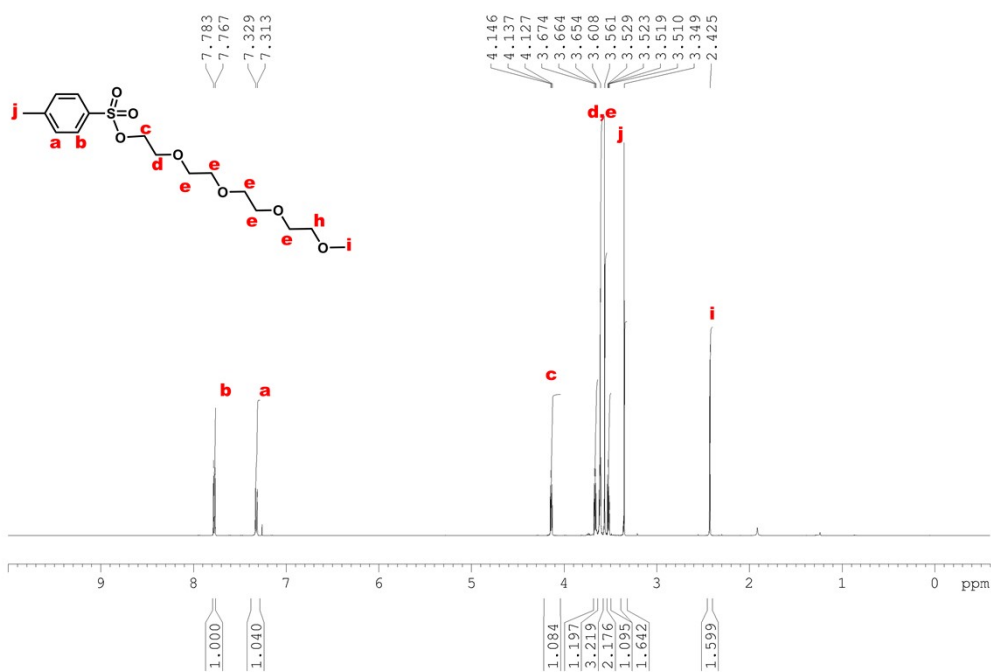


**Fig. S3.**  $^1\text{H}$  NMR spectrum of **TEG-OTs** in  $\text{CdCl}_3$ .

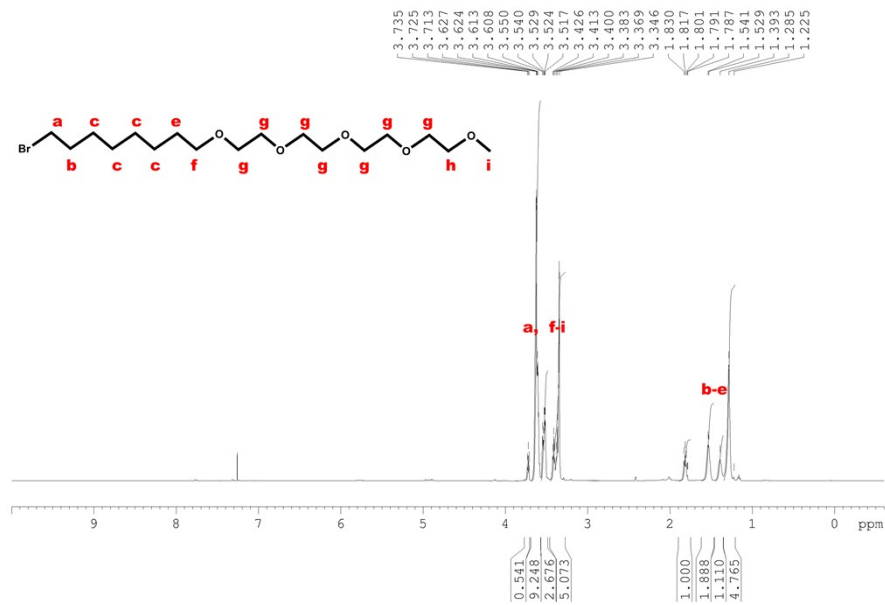


Fig. S4.  $^1\text{H}$  NMR spectrum of TEG-C8-Br in  $\text{CdCl}_3$ .

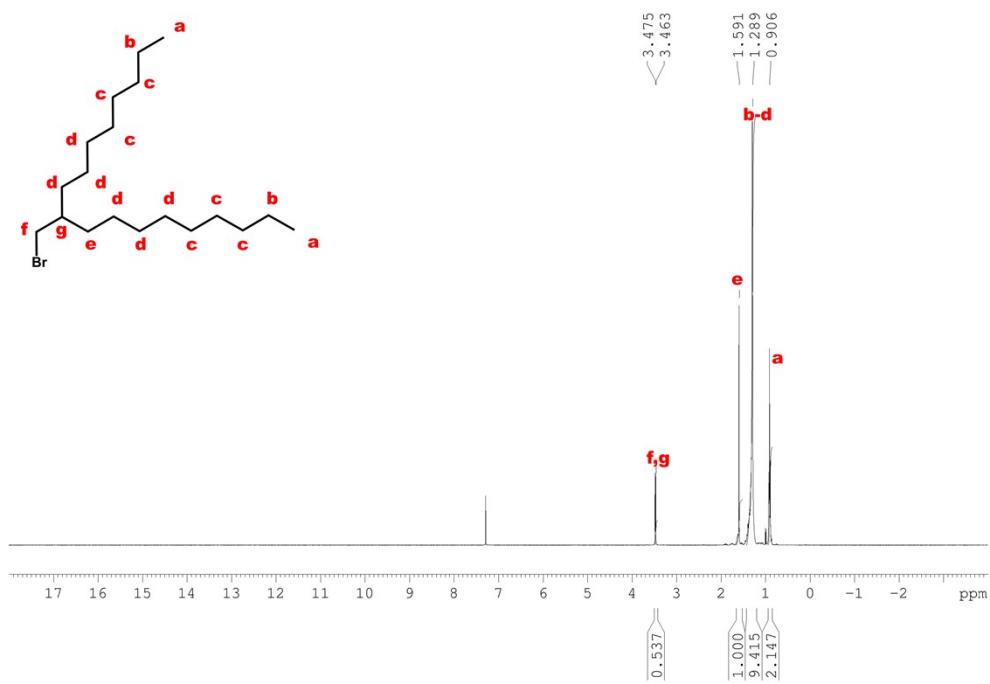
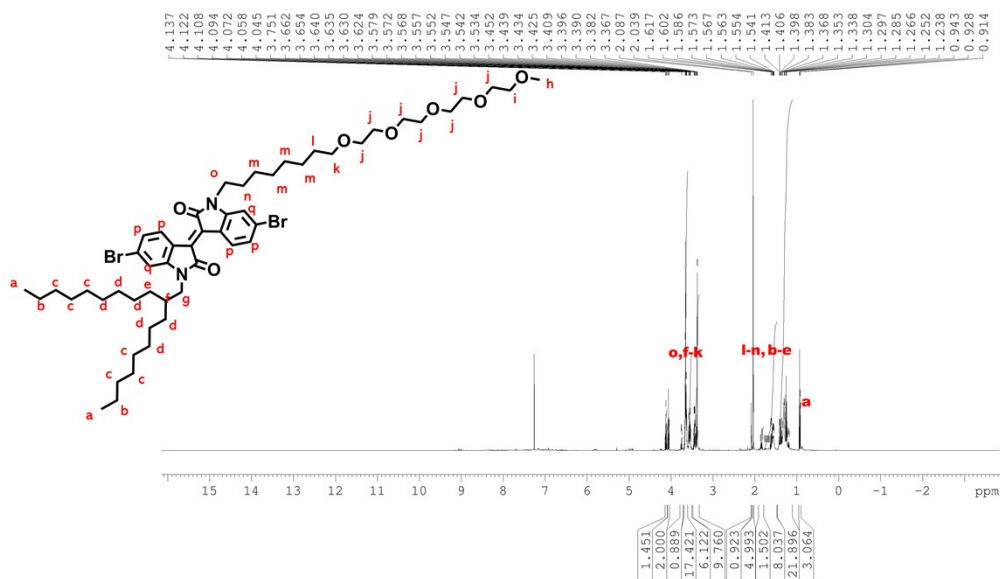
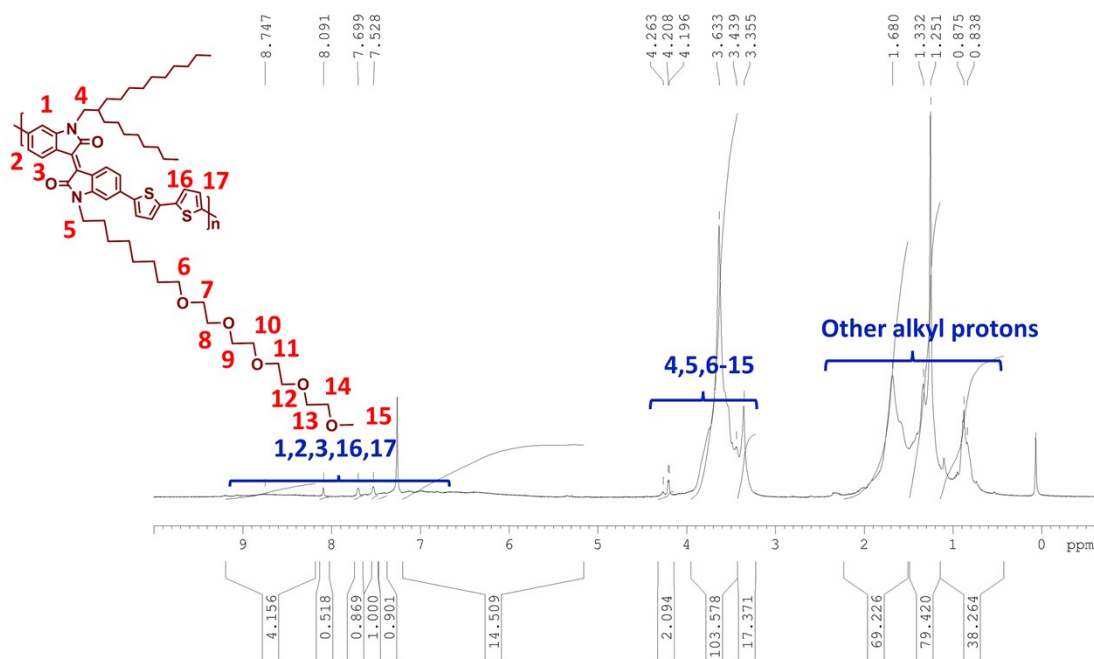


Fig. S5.  $^1\text{H}$  NMR spectrum of OD-Br in  $\text{CdCl}_3$ .



**Fig. S6.**  $^1\text{H}$  NMR spectrum of **M(C,O)** in  $\text{CdCl}_3$ .



**Fig. S7.**  $^1\text{H}$  NMR spectrum of **P(C,O)** in  $\text{CdCl}_3$ .



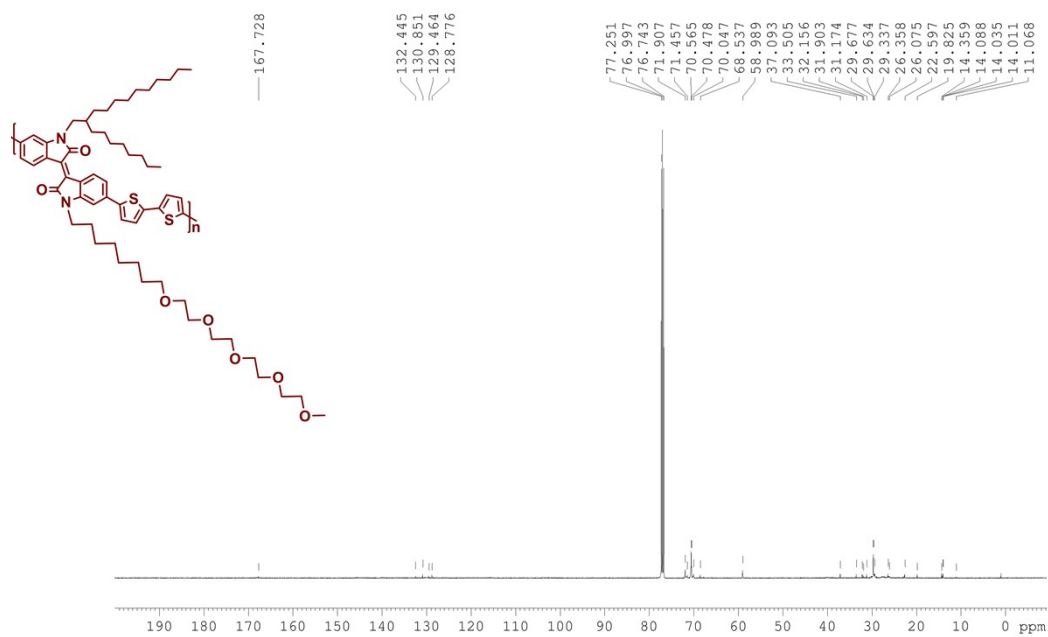


**Fig. S8.**  $^{13}\text{C}$  NMR spectrum of P(C,O) in  $\text{CdCl}_3$ .

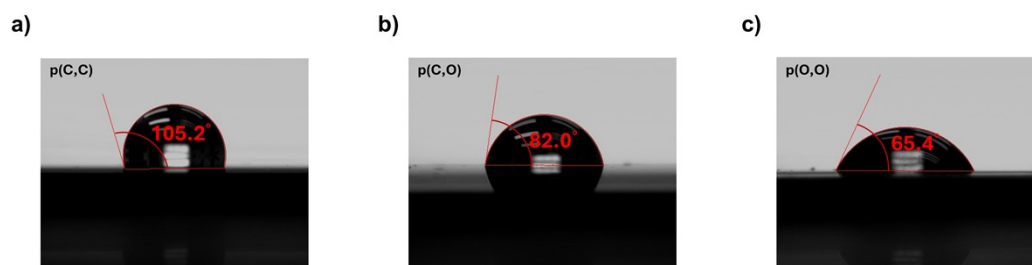


**Fig. S9.** Contact angle measurements of water droplets on the polymer films: (a) P(C,C), (b) P(C,O), and (c) P(O,O).

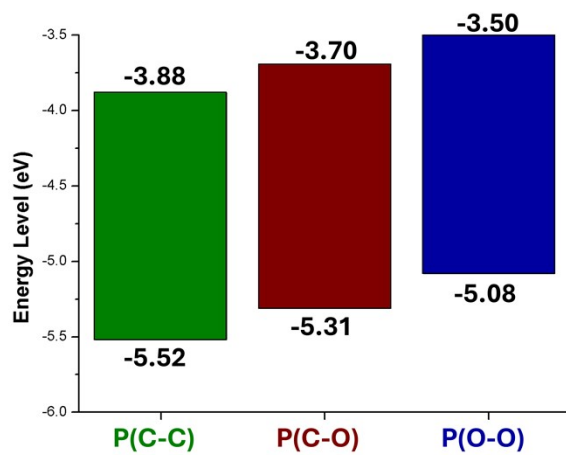


**Fig. S10.** Frontier energy level diagram of the polymers studied.

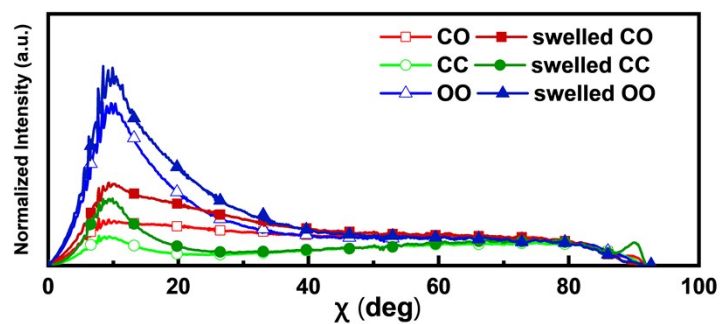


**Fig. S11.** Geometrically corrected pole figures of the polymer films derived from the azimuthal integral of their (100) diffractions in 2D GIXD patterns.

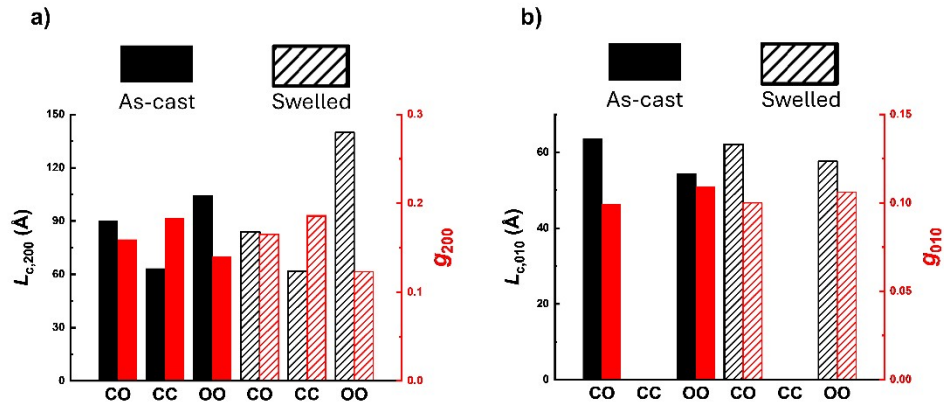


**Fig. S12.** Summary of the crystallographic parameters:  $L_c$  and  $g$  of (a) (200) diffractions and (b) (010) diffractions of the as-cast and electrolyte-swelled polymer films.

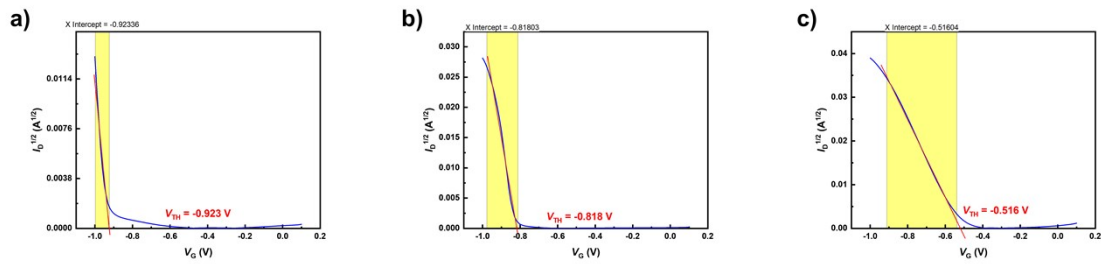


**Fig. S13.** The relationship of  $I_d^{1/2}$  vs.  $V_g$  of (a) P(C,C), (b) P(C,O), and (c) P(O,O) based OECT devices.

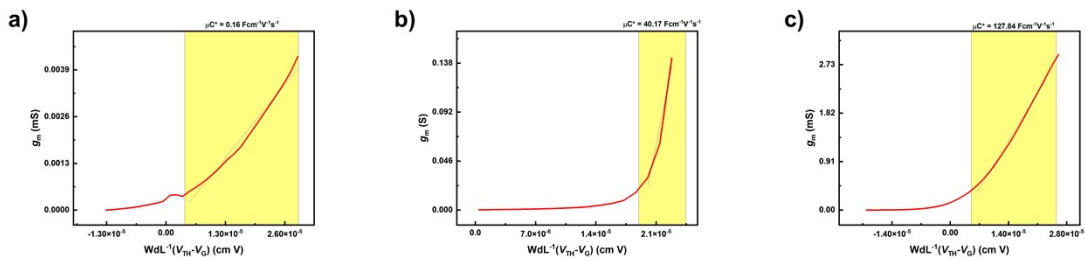


**Fig. S14.** The relationship of  $g_m$  vs.  $WdL^{-1}(V_{th} - V_g)$  of (a) p(C,C), (b) p(C,O), and (c) P(O,O) based OECT devices.

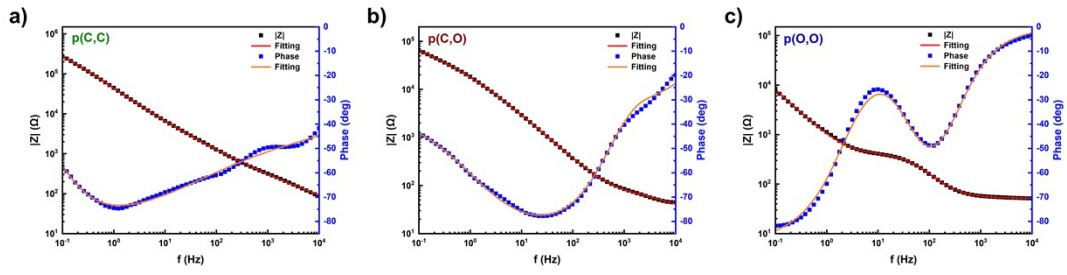


**Fig. S15.** Bode plots derived from the EIS characteristics of the polymer films: (a) P(C,C), (b) P(C,O), and (c) P(O,O).

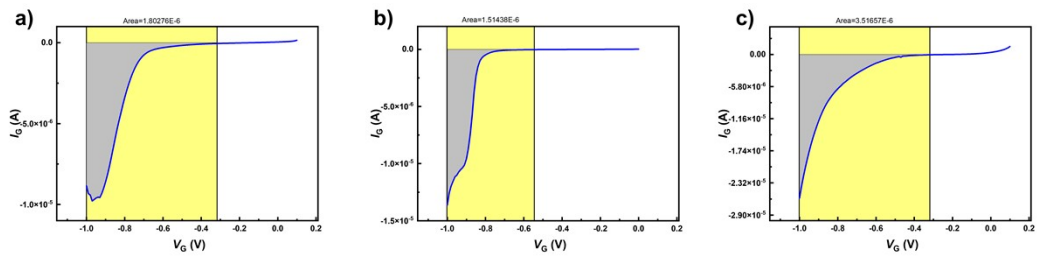


**Fig. S16.** The relationship of  $I_g$  vs.  $V_g$  of (a) P(C,C), (b) P(C,O), and (c) P(O,O) based OECT devices.

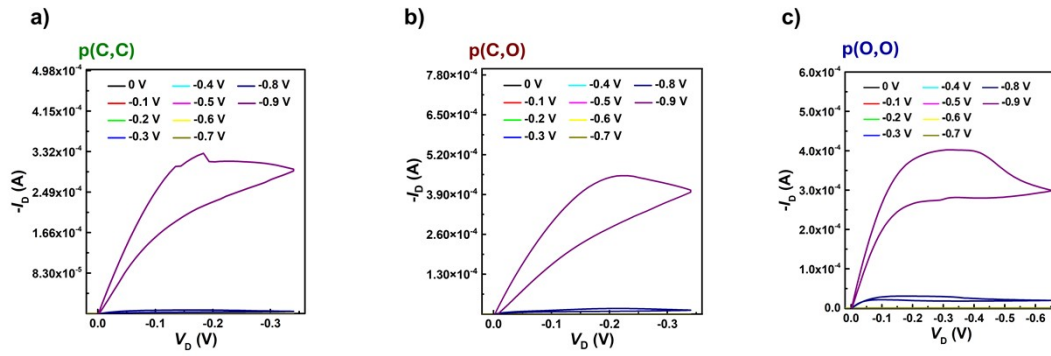


**Fig. S17.** Output characteristics of (a) P(C,C), (b) P(C,O), and (c) P(O,O) based OECD devices with a forward  $V_D$  sweeping from 0 to  $-0.3 \sim -0.6$  V at  $V_G = 0 \sim -0.9$  V.

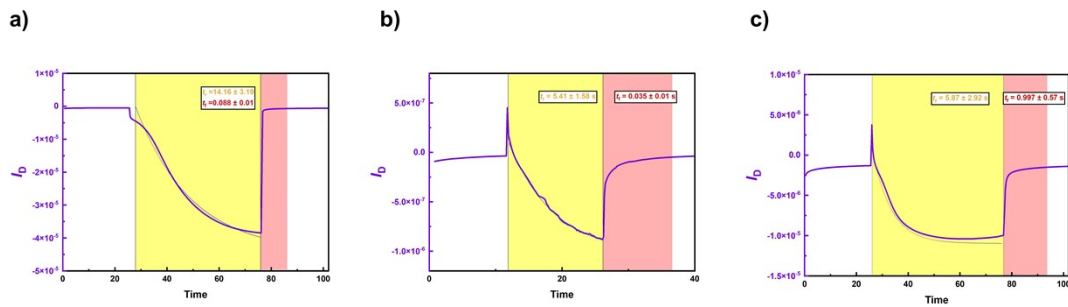


**Fig. S18.** Transient curves of (a) P(C,C), (b) P(C,O), and (c) P(O,O) based OECD devices. The x (time) and y ( $I_D$ ) axes are in units of [s] and [A]. The exponential fittings indicate their characteristic response time.

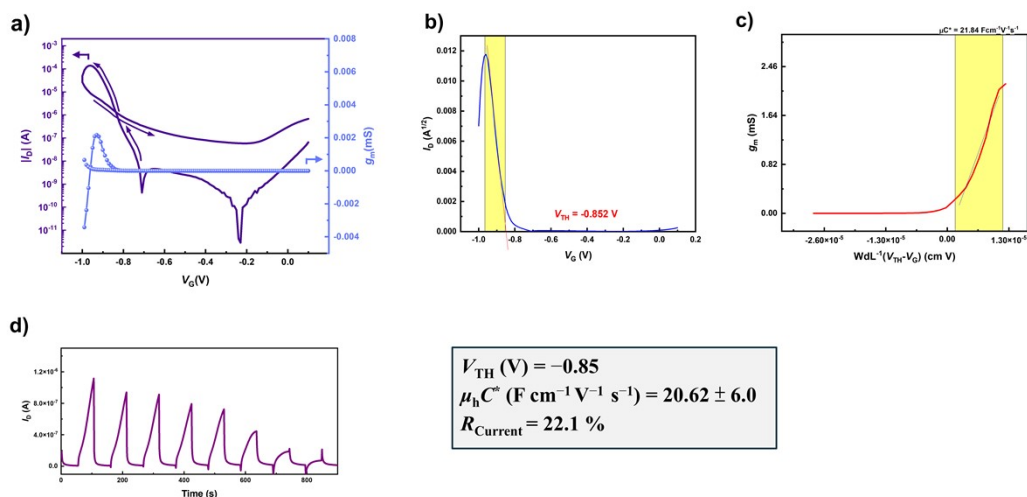


**Fig. S18.** OECT transfer characteristics of the reference device comprising the polymer blend of P(C,C) and P(O,O): (a) Transfer curve with a forward  $V_G$  sweeping from 0.1 to  $-1.0$  V at  $V_D = -0.3$  V. (b) The relationship of  $I_d^{1/2}$  vs.  $V_g$ . (c) The relationship of  $g_m$  vs.  $WdL^{-1}(V_{th} - V_g)$ . (d) Transient characteristics of the polymer films with  $V_G$  pulse of  $-0.85$  V at  $V_D = -0.3$  V for 8 cycles.